



Enrichment Virtual Screening, ADME and Molecular Simulation Studies of Potential Inhibitors of Human c-Myc Protein in Multiple Myeloma

Ayodele Sunday Alonge¹ , Toluwase Hezekiah Fatoki^{2,*} , Courage Dele Famusiwa³ ,
Iseoluwa Isaac Ajayi¹ , Jude Akinyelu⁴ , Akinwunmi Oluwaseun Adeoye³ ,
Emmanuella Chidinma Nwokporo¹ 

¹ Department of Biological Sciences, School of Life Science, Bamidele Olumilua University of Education, Science and Technology Ikere-Ekiti, Ekiti State, Nigeria; alonge.ayodele@bouesti.edu.ng (A.S.A); ajayi.isaac@bouesti.edu.ng (I.I.A); nwokporochidinma60@gmail.com (E.C.N);

² Applied Bioinformatics Laboratory, Department of Biochemistry, Faculty of Science, Federal University Oye-Ekiti, Ekiti State, Nigeria; toluwase.fatoki@fuoye.edu.ng (T.H.F);

³ Phytomedicine and Molecular Toxicology Research Laboratory, Department of Biochemistry, Faculty of Science, Federal University Oye-Ekiti, Ekiti State, Nigeria; courage.famusiwa@fuoye.edu.ng (C.D.F);
akinwunmi.adeoye@fuoye.edu.ng (A.O.A);

⁴ Nanobiochemistry Research Laboratory, Department of Biochemistry, Faculty of Science, Federal University Oye-Ekiti, Ekiti State, Nigeria; jude.akinyelu@fuoye.edu.ng (J.A);

* Correspondence: toluwase.fatoki@fuoye.edu.ng;

Received: 30.05.2025; Accepted: 6.10.2024; Published: 6.09.2025

Abstract: The c-Myc proto-oncogene, a frequently activated oncogene implicated in approximately 20% of human cancers, including incurable multiple myeloma (MM), leads to the formation of a c-Myc-Max molecular complex. This complex recognizes and binds to DNA E-box sequences, recruiting the necessary transcriptional machinery to activate or repress specific target genes. Consequently, inhibiting the c-Myc-Max interaction or disrupting c-Myc stability with small molecules emerges as a promising strategy to repress the c-Myc function. The methods used are enrichment virtual screening, pharmacokinetics, docking, and molecular dynamic (MD) simulation. A total of 8 compounds with high gastrointestinal absorption, resistance to P-glycoprotein (P-gp), some permeability through the blood-brain barrier, and minimal inhibitory effects on selected cytochrome P450s were obtained. For c-Myc and c-Myc-Max, (-)-Epigallocatechin gallate (KDH) has a binding affinity of $-5.056 \text{ kcal.mol}^{-1}$ and $-6.391 \text{ kcal.mol}^{-1}$ respectively, while (+)-Catechin 3-Gallate (XEG) has $-4.754 \text{ kcal mol}^{-1}$ and $-6.512 \text{ kcal.mol}^{-1}$ respectively. MD simulation showed suitable protein-ligand stability, and the interactions of c-Myc-Max with XEG were better than those of KDH. This study showed that c-Myc activity or c-Myc/Max interaction could be modulated either by catalytic inhibition or poison by intercalation. Further investigations are imperative to validate the efficacy of the results of this study.

Keywords: c-Myc-Max; cancer; ChEMBL1077108 (Furospogolide); ChEMBL464381 (Palinurin); ChEMBL284377 (Dexfosfoserine); pharmacokinetics; molecular docking; molecular dynamics simulation.

© 2025 by the authors. This article is an open-access article distributed under the terms and conditions of the Creative Commons Attribution (CC BY) license (<https://creativecommons.org/licenses/by/4.0/>), which permits unrestricted use, distribution, and reproduction in any medium, provided the original work is properly cited. The authors retain copyright of their work, and no permission is required from the authors or the publisher to reuse or distribute this article, as long as proper attribution is given to the original source.

1. Introduction

The c-Myc proto-oncogene, a member of the basic helix-loop-helix leucine zipper (bHLH-LZ) family capable of activating or repressing gene expression, stands out as one of the most frequently activated oncogenes, implicated in an estimated 75% of all human cancers, including breast, cervical, colon and prostate cancers, lymphomas, neuroblastoma, myeloid leukemia, and small-cell lung carcinomas, among others, most oftentimes, they are found aggressive and irresponsive to the current therapies [1]. Notably, It can regulate up to 15% of genes across species, particularly affecting specific gene classes related to metabolism, protein biosynthesis, cell cycle regulation, cell adhesion, and the cytoskeleton [2,3].

The c-MYC protein consists of a DNA binding domain followed by a bHLH-LZ motif at the C-terminal. This DNA binding domain serves as the site for c-MYC's heterodimerization with its partner molecule, the transcription factor Myc-associated factor X (Max). Elevated c-Myc protein levels result in heterodimerization with Max, forming the c-Myc/Max partnership. This complex can then recognize and bind to DNA E-box sequences, recruiting the transcriptional machinery necessary to activate or repress specific target genes [2, 4-6]. The c-Myc-Max-Miz-1 complex plays a role in repressing cell cycle inhibitors such as CDK inhibitor p15Ink4b (CDKN2B) and is implicated in preventing cell growth inhibition [7]. c-Myc is involved in the pathogenesis of a significant number of malignancies, approximately 60-70% of solid and hematopoietic tumors [8] and multiple myeloma (MM), a common incurable hematological tumor [9].

Multiple myeloma (MM) is a B-cell neoplasm resulting from the clonal proliferation of plasma cells in the bone marrow, which produce monoclonal immunoglobulins (M-protein) that could be trapped within some organs such as bone and kidney, thereby causing progressive dysfunction, with symptoms which include anemia, hypercalcemia, osteolytic bone disease, or renal failure [10-12]. In MM, c-Myc acts as a primary oncogene [13]. According to Gupta et al. [14], MM cells binding to bone marrow cells stimulate the production of various cytokines, including interleukin-6, interferon-gamma, vascular endothelial growth factor, tumor necrosis factors, transforming growth factor- β , and receptor activator of nuclear factor- κ B ligand. The emerging therapies for the management of MM in both newly diagnosed and relapsed and/or refractory patients include bortezomib, carfilzomib, pomalidomide with or without low-dose dexamethasone, a compound targeting B-cell maturation antigen, and chimeric antigen receptor T-cells, and others [11, 12, 15-17].

c-Myc regulates a significant portion of genes (up to 15%) through two mechanisms: (i) activation of gene transcription by c-Myc/Max heterodimers binding to specific recognition sites (E-box elements) within promoter regions and (ii) repression of c-Myc-regulated genes via indirect recruitment of c-Myc/Max dimers to DNA through the zinc-finger protein Miz-1 [18]. To inhibit c-Myc functions, blocking the protein-protein interactions essential for c-Myc and Max association, irrespective of DNA presence, is crucial [18].

Targeting oncogenic Myc for antitumor effects in cancer treatment has been investigated by indirect approach of blockade Myc to achieve Myc destabilization, disruption of Myc/Max complex, inhibition of MYC transcription and/or translation, and synthetic lethality associated with Myc overexpression [19-21]. Indirect approaches aim to disrupt c-Myc stability; compounds like oridonin induce E3 ligases FBW7 and Skp2, promoting c-Myc degradation [22]. Eukaryotic initiation factor-4A (eIF4A) targeted by Silvestrol and Src kinase

targeted by saracatinib also show promise in reducing c-Myc translation rates and impairing tumor development [23,24]. Targeting c-Myc/Max interaction remains an appealing approach.

In silico enrichment, virtual screening could be used for c-Myc or c-Myc/Max modulator discovery due to its efficiency, cost-effectiveness, target specificity, and iterative refinement, while limitations include potential inaccuracies, simplified models, and the need for advanced computational assessment such as pharmacokinetic and target prediction, molecular docking, molecular dynamics simulation with binding energy calculation, and ultimately experimental validation. Moreover, biophysical and computational approaches have been deployed to investigate a new set of inhibitors of c-Myc [25-30]. Some promising low molecular weight MYC inhibitors that have been discovered include MYCMI-6, PKUMDL-YC-1205, KJ-Pyr-9, MYC975, KSI-3716, and many others [1, 20, 27, 31]. Thus, this study aimed to identify potential c-Myc or c-Myc/Max modulators through *in silico* enrichment virtual screening, pharmacokinetics, docking, and MD simulation.

2. Materials and Methods

2.1. Protein-protein interaction analysis.

The human Myc proto-oncogene (c-Myc) protein (UniProt ID: P01106, Gene ID: MYC) sourced from the UniProt database (www.uniprot.org) was utilized. Protein-protein interaction (PPI) profiling was conducted using the STRING webserver v12.0 (<https://string-db.org/>, [32]) using the gene ID: MYC.

2.2. Enrichment virtual screening.

The UniProt ID was employed for enrichment virtual screening on the LIGQ webserver (ligq.qb.fcen.uba.ar) with the full pipeline setting. LIGQ generated a compound set with binding evidence to the input protein or similar ones based on prior biological assays [33].

2.3. Clustering analysis.

Sets of ligands in SMILES format underwent scrutiny, removing non-druglike molecules. Clustering analysis with multidimensional scaling was performed on the ChemMine server (<http://chemmine.ucr.edu/>) [34] using the ligands' SMILES.

2.4. *In silico* ADME prediction.

In silico ADME (absorption, distribution, metabolism, and excretion) screening for compounds was conducted on the SwissADME server (www.swissadme.ch) at default parameters using the SMILES format [35]. Duplicated ligands were excluded from subsequent analyses.

2.5. Molecular docking.

The ligands' SMILES underwent 3D structure optimization using ACDLab/Chemsketch software and were saved in .mol format. Subsequently, PyMol software facilitated the conversion of ligand files from .mol to .pdb format. The c-Myc 3D structure was obtained in AlphaFold PDB format from the UniProt database (AlphaFold ID: AF-P01106), and the 3D structure of c-Max/Max was obtained from the protein database (PDB ID: 1NKP). Prior to docking, ligands and target protein structures in PDB format were formatted to PDBQT

using AutoDock Tools (ADT) v1.5.6 [36]. Ligand-protein molecular blind docking, which sampled all the binding pockets present on the protein instead of just the active site alone, was executed using AutoDock Vina v1.2.3 [37,38], as previously reported [39,40]. Binding affinity and close interactions between ligands and targets were analyzed and visualized using ezLigPlot on the ezCADD webserver at <http://dxulab.org/software> [41].

2.6. Molecular dynamics simulation.

Molecular dynamics simulations, lasting 100 nanoseconds, were conducted using Desmond from Schrodinger suite v2018-3 [40,42,43]. Protein and ligand complex configurations for molecular dynamics simulation were derived from docking studies. The complexes underwent preprocessing, including optimization and minimization, using Maestro's protein preparation wizard. Systems were prepared using the System Builder tool, selecting the TIP3P Solvent Model with an orthorhombic box. The simulation employed the OPLS-2005 force field, and neutralization was achieved by adding 0.15 M NaCl counter ions to mimic physiological conditions [44]. The NPT ensemble with a temperature of 310 K and pressure of 1 atm was selected for the entire simulation. Models were relaxed before simulation, and trajectories were saved every 100 ps. Post-simulation analysis included determining root-mean-square deviation (RMSD), root-mean-square fluctuation (RMSF), and protein-ligand interaction profiles. Additionally, prime molecular mechanics/generalized Born surface area (MMGBSA) calculations were conducted to determine the binding free energy (ΔG_{bind}) [40,42,45] as follows:

$$\text{MMGBSA } \Delta G_{bind} = \Delta G_{\text{Coulomb}} + \Delta G_{\text{Covalent}} + \Delta G_{\text{Hbond}} + \Delta G_{\text{Lipo}} + \Delta G_{\text{Packing}} + \Delta G_{\text{SolvGB}} + \Delta G_{\text{vdW}} \quad (1)$$

3. Results and Discussion

This study successfully identified several structurally diverse small-molecule inhibitors of c-Myc through screening, with potential for disrupting c-Myc protein-protein interactions. The enrichment virtual screening of the LIGQ web server is based on the capacity to detect known binders and potential binders to a desired target and extend the list by selecting a small set of commercial compounds enriched in potential binders from a large database of commercially available compounds using a chemical similarity cutoff [33].

In this study, protein-protein interaction of human c-Myc protein was predicted, and the results showed that its primary interacted proteins are MAX (protein max), EP300 (histone acetyltransferase p300), BIN1 (Myc box-dependent-interacting protein 1), TRRAP (transformation/transcription domain-associated protein), ZBTB17 (zinc finger and BTB domain-containing protein 17), BRCA1 (breast cancer type 1 susceptibility protein), FBXW7 (F-box/Wd repeat-containing protein 7), CDKN2A (cyclin-dependent kinase inhibitor 2A), TP53 (cellular tumor antigen p53) and KAT2A (histone acetyltransferase KAT2A) as shown in Figure 1. Some of the identified proteins that directly interact with c-Myc were predicted in this study, which include TP53, EP300, BRCA1, Fbxw7, and TRRAP, showing the indispensability of c-Myc in cancer diseases [31]. Notably, the transformation/transcription domain-associated protein (TRRAP), a crucial c-Myc co-factor, forms STAGA complexes with histone acetyltransferase (HAT) activity [46]. Additionally, transcriptional co-factors p300 and cyclic AMP response element-binding protein (CBP) interact with c-Myc at two distinct sites, influencing its transactivating activity and acting as an activator [47,48].

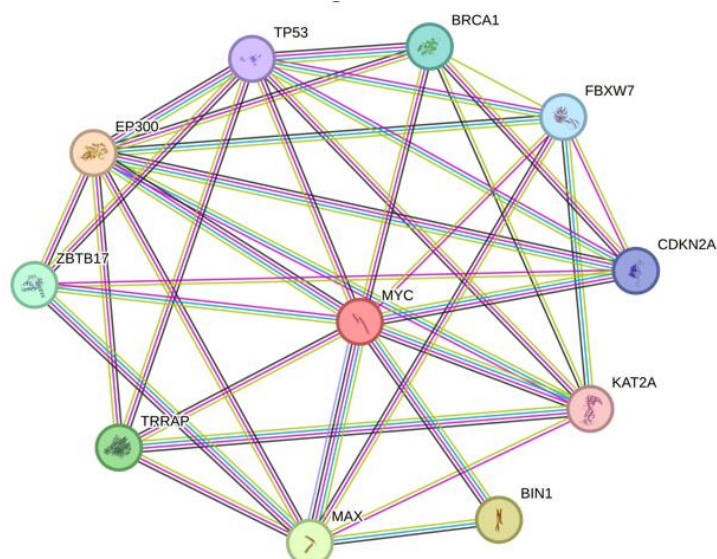


Figure 1. Protein-protein interaction profile of MYC.

The inhibition of c-Myc in small-cell lung cancer has been linked to the inactivation of the TP53 gene [49]. About 6-8% of cases of MM have been associated with TP53 mutation, but mutation-targeted therapeutic intervention in MM has been unsuccessful due to intra-clonal heterogeneity and subclonal complex structure, impacted by bone marrow, immune response, and therapy [11].

Studies indicate that c-Myc plays a pivotal role in increasing the intracellular iron pool, enhancing glucose uptake, glycolysis, and nucleotide synthesis, as well as regulating RNA polymerase I and polymerase III transcription for ribosome biogenesis and protein synthesis [50-53]. Deregulated c-Myc expression contributes to apoptosis under nutrient or growth factor deprivation, mediated by NRF-1 target genes [54,55]. c-Myc neoplasia often involves cooperation with other oncogenic agents, leading to the loss of regulatory checkpoints and feedback loops [56].

The c-Myc/Max dimers have been shown to repress transcription by disrupting the association of Miz1 with the p300 coactivator, suggesting a role for Max in transcriptional regulation beyond previous understanding [57-59]. The HBP1 transcriptional repressor, a suppressor of Wnt signaling, also inhibits the expression of endogenous Wnt gene targets Cyclin D1 and c-Myc. Notably, (-)-epigallocatechin-3-gallate (EGCG), a major green tea phytochemical, blocks Wnt signaling through HBP1 transcriptional repression [60].

Complicating matters, c-Myc, a nuclear protein lacking enzymatic function, has a history of poor interaction with small molecules [61]. Directly targeting c-Myc is challenging, as it is considered undruggable due to its disordered nature and the absence of identifiable stable druggable pockets and cavities [58,62]. The development of improved c-Myc/Max inhibitors for assessing new clinical anti-cancer therapies has greatly benefited from detailed structural models of c-Myc/small molecule interactions [63].

The rational enrichment virtual screening was done on the c-Myc protein to determine a set of compounds that could modulate it. The results of the virtual screening gave a total of 15 compounds in SMILES format (Supplementary Table S1). The 15 compounds were subjected to hierarchical clustering, which revealed their structural similarities based on their physicochemical properties, as shown in Figure 2. Clustering results showed the structural similarities of the identified compounds based on physicochemical properties, but it does not guarantee similar biological effects because variation in functional groups could impact

significant therapeutic outcomes. For instance, (+)-Catechin 3-Gallate (XEG) differs from (-)-Epigallocatechin gallate (KDH) by a single hydroxyl group and optical configuration that alters the function as predicted in this study.

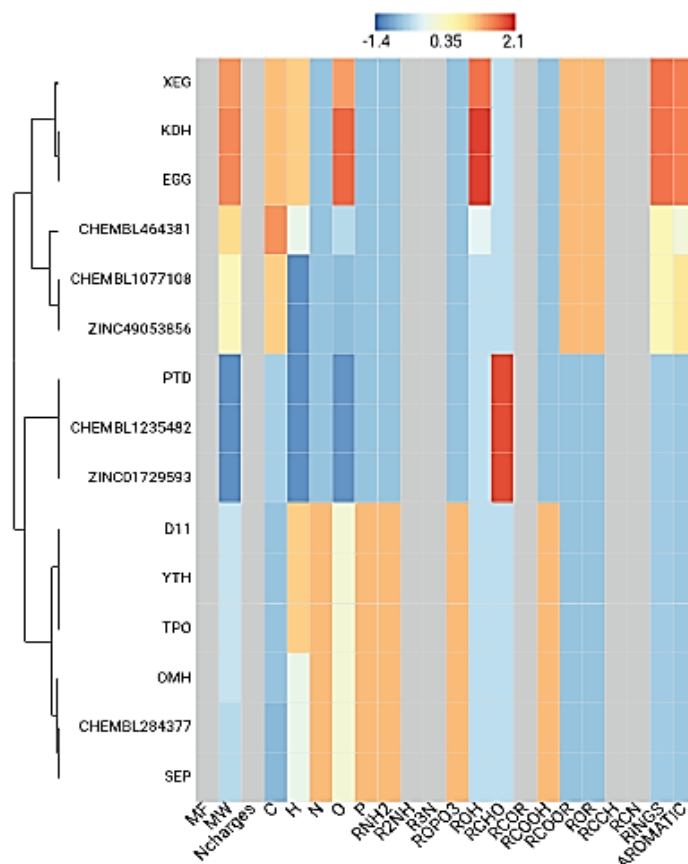


Figure 2. Hierarchical clustering results. Parameter options used are heatmap (distance matrix); Linkage Method (single); physicochemical properties heatmap (chemmineR properties), and properties color and display values (Z-scores).

Also, the 15 compounds were subjected to pharmacokinetic prediction, and the results were manually checked of which compounds were duplicated, and those with low gastrointestinal absorption (GIA) were removed, and a total of 8 compounds were obtained (Table 1). These compounds were not a substrate of P-glycoprotein (P-gp), while some of the compounds were permeant of the blood-brain barrier (BBB), had good solubility, and very few had an inhibitory effect on the selected cytochrome P450s (Table 2). The pharmacokinetic properties showed that CHEMBL1077108 (Furospongolide) and CHEMBL464381 (Palinurin) have moderate solubility, high gastrointestinal absorption (GIA), cross the blood-brain barrier (BBB) and inhibit some cytochrome P450s. These properties are good for oral drug administration, and they are less affected by first-pass metabolism, so they could be present as neuroactive effects.

Table 1. Identified ligand structure and name.

S. No.	Ligand code	Compound structure	Common name	PubChem CID
1	TPO		O-phospho-L-threonine, phosphothreonine	3246323
2	CHEMBL1077108, ZINC49053856		Furospongolide	21637526

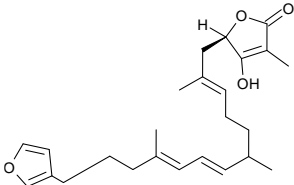
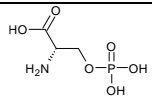
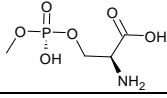
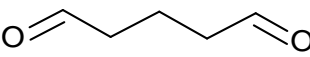
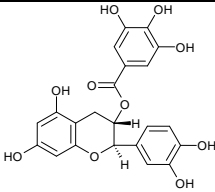
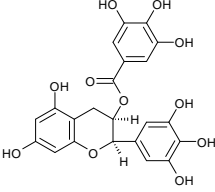
S. No.	Ligand code	Compound structure	Common name	PubChem CID
3	CHEMBL464381		Palinurin	54726684
4	CHEMBL284377, SEP		O-phospho-L-serine; Dexfosfoferine	68841
5	OMH		O-[(S)- hydroxy(methoxy)phosphoryl]- L-serine	49867438
6	CHEMBL1235482, ZINC01729593, PTD		Pentanedial	3485
7	XEG		(+)-Catechin 3-Gallate	5276454
8	KDH, EGG		(-)-Epigallocatechin gallate (EGCG)	1016

Table 2. Predicted pharmacokinetics of the compounds.

SN	Ligands ID	Predicted ADME Parameter from SWISSADME											
		MW	MR	TPSA (Å ²)	Log P	ESOL Log S	ESOL Class	GIA	BBB permeant	P-gp	CYPs Inhibitor	Lip	BS
1	TPO	199.1	37.89	139.89	-2.56	2.16	Highly soluble	Low	No	No	None	0	0.56
2	CHEMBL 1077108	328.45	98.34	39.44	4.94	-4.72	Moderately soluble	High	Yes	No	CYP2C19, CYP2C9, CYP2D6, CYP3A4	0	0.55
3	CHEMBL 464381	398.54	118.66	59.67	4.86	-4.72	Moderately soluble	High	Yes	No	CYP2C19, CYP2C9, CYP2D6	0	0.55
4	CHEMBL 284377	185.07	33.09	139.89	-2.7	2.12	Highly soluble	Low	No	No	None	0	0.56
5	OMH	199.1	37.82	128.89	-2.31	2.16	Highly soluble	High	No	No	None	0	0.56
6	CHEMBL 1235482	100.12	26.55	34.14	0.38	0.15	Highly soluble	High	Yes	No	None	0	0.55
7	XEG	442.37	110.04	177.14	1.28	-3.7	Soluble	Low	No	No	None	1	0.55
8	KDH	458.37	112.06	197.37	0.95	-3.56	Soluble	Low	No	No	None	2	0.17

Physicochemical properties: Molecular weight (MW); Molar Refractivity (MR); Total polar surface area (TPSA); **Lipophilicity:** Consensus Log P; **Water Solubility:** ESOL Log S, ESOL Class; **Pharmacokinetics:** Gastrointestinal absorption (GIA); Blood-brain barrier (BBB); P-glycoprotein (P-gp) substrate; Inhibition of Cytochrome P450 (CYPs) type CYP1A2, CYP2C19, CYP2C9, CYP2D6, and CYP3A4; **Druglikeness:** Lipinski (Lip), Bioavailability Score (BS); **Medicinal Chemistry:** Synthetic accessibility (SA).

Moreover, although XEG and KDH differ by a hydroxyl group, the KDH violated two of Lipinski's rules, which affected their lipophilicity (Log P) and bioavailability. Ligands violating two or more conditions may exhibit inadequate absorption and permeability. Drug toxicity decreases with a decrease in lipophilicity (Log P value) because the higher the lipophilicity, the lesser the solubility [64]. Less solubility in water has been observed for novel

inhibitors of c-Myc, but compound PKUMDL-YC-1205 has been reported to have high water solubility [27]. Small molecule inhibitors of c-Myc, like IIA6B17, 10058-F4, 10074-G5, and JY-3-094, suffer from low bioavailability and poor cell penetration [65].

CHEMBL1077108 (Furospogolide) antitumor effect has been linked to inhibition of hypoxia-inducible factor-1 (HIF-1) induction in breast tumor cells [66], CHEMBL464381 (Palinurin) was found to inhibit GSK-3B in human neuroblastoma cells [67], while CHEMBL284377 (Dexfosfoserine) is an amino acid, a phosphoric acid ester of serine, used for nutritional supplementation therapy in over-fatigue condition, often combined with cyanocobalamin and L-glutamine (Ref: www.drugbank.ca). Green tea polyphenols, including EGCG and ECG, have been shown to modulate the expression of genes associated with pulmonary hyperplasia, dysplasia, and lung cancer development [68,69]. EGCG has been associated with mitigating metabolic changes in cancers such as prostate cancer by modulating the PI3K/Akt/mTOR pathway [70]. Phytochemicals from medicinal plants have been exploited for direct modulation of c-Myc activities. For example, celastrol has been shown to bind c-Myc/Max to abrogate E-box binding [71].

The SMILES of the 8 compounds were checked on the PubChem database, and their PubChem CIDs were obtained. The 8 compounds were subjected to molecular docking analyses against the three-dimensional structure of c-Myc and c-Myc/Max, respectively, and the results of binding affinity are presented in Table 3. The result showed that KDH (PubChem CID: 1016) has a binding affinity of $-5.056 \text{ kcal mol}^{-1}$ and $-6.391 \text{ kcal mol}^{-1}$ for c-Myc and c-Myc/Max respectively, while compound XEG (PubChem CID 5276454) has $-4.754 \text{ kcal mol}^{-1}$ and $-6.512 \text{ kcal mol}^{-1}$ for c-Myc and c-Myc/Max respectively, which are better than that of Doconexen which is a standard drug (Table 3). These results showed that compounds KDH, XEG, TPO, and CHEMBL284377 have better binding affinity for c-Myc/Max than c-Myc.

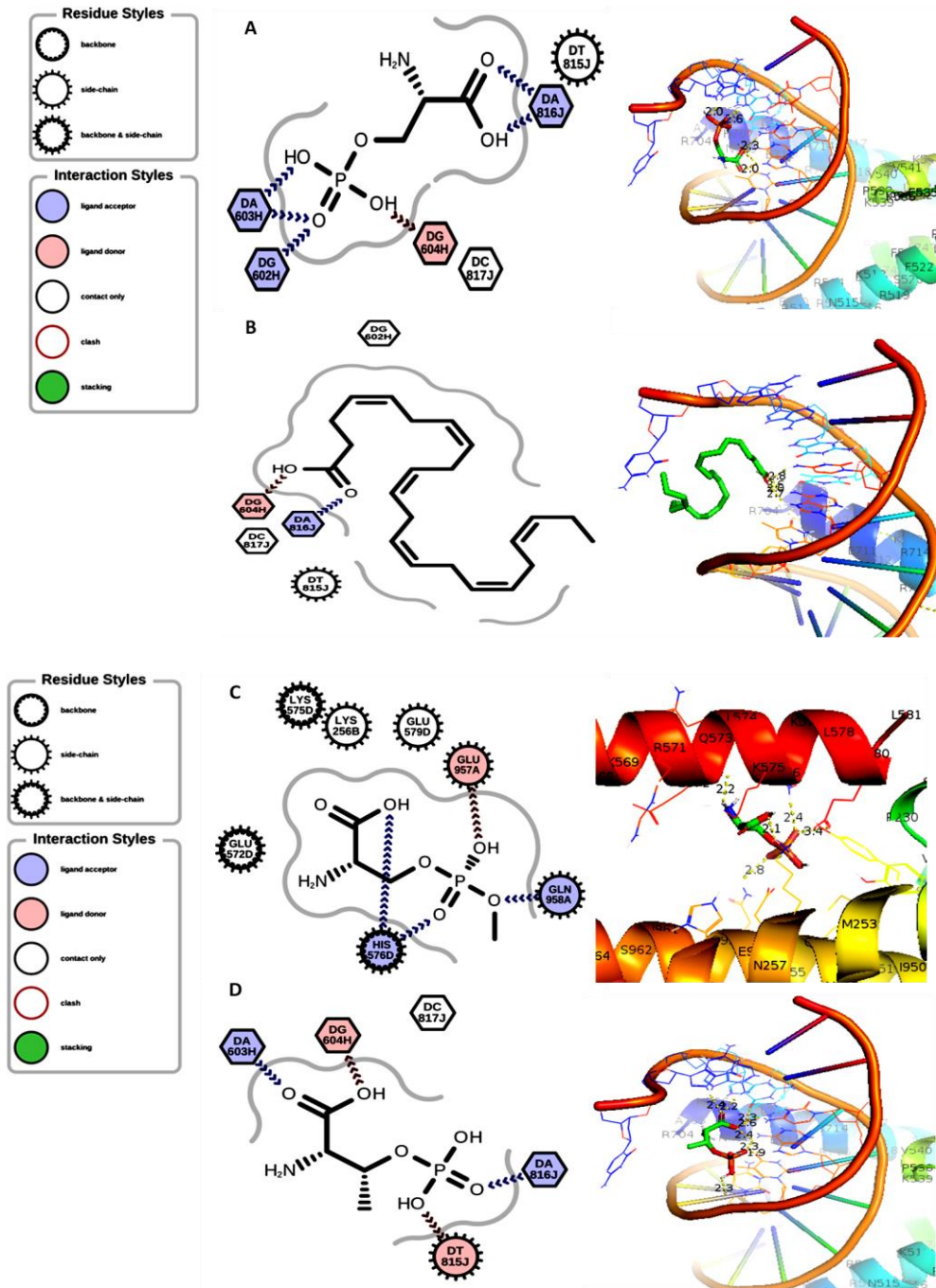
CHEMBL284377, Doconexen, TPO and KDH bind to c-Myc/Max. On the DNA, the helix bases are not amino acids, whereas OMH and XEG bind to c-Myc/Max. It is on the amino acids, not DNA helix bases. The binding pose of the complex with high binding affinity is presented in Figure 3, which shows the amino acid residues or nucleotide bases involved in the binding interaction. For c-Myc, amino acid residues CYS117, ALA140, GLU253, and GLU388 serve as ligand hydrogen donors, while GLU255 serves as a ligand hydrogen acceptor. For c-Myc/Max, the ligand hydrogen acceptors are amino acid residues GLN958, HIS576, and nucleotide bases dA603, dG602, dA816 while the ligand hydrogen donors are amino acid residues GLU957, GLU572, GLN580, and nucleotide bases dG604, and dT815.

Table 3. Docking results of the compounds against c-Myc and c-Myc/Max.

S. No	Ligands	PubChem CID	c-Myc (AlphaFold ID: AF-P01106) Binding Affinity ΔG (kcal.mol ⁻¹)	c-Myc/Max (PDB ID: 1NKP) Binding Affinity ΔG (kcal.mol ⁻¹)
1	TPO	3246323	-3.403	-4.977
2	CHEMBL 1077108	21637526	-3.943	-3.196
3	CHEMBL 464381	54726684	-4.014	-3.609
4	CHEMBL 284377	68841	-3.095	-5.117
5	OMH	49867438	-3.139	-4.626
6	CHEMBL 1235482	3485	-2.766	-3.406

7	XEG	5276454	-4.754	-6.512
8	KDH	1016	-5.056	-6.391
9	Doconexent (standard)	445580	-3.124	-3.391

Docking parameter: c-Myc (UniProt ID: P01106) [spacing: 1.000, npts: 126 × 126 × 126, center: 6.333 × 1.024 × -12.133]. c-Myc/Max (PDB ID: 1nkp) [spacing: 1.000, npts: 126 × 126 × 126, center: 53.479 × 47.625 × 57.374].



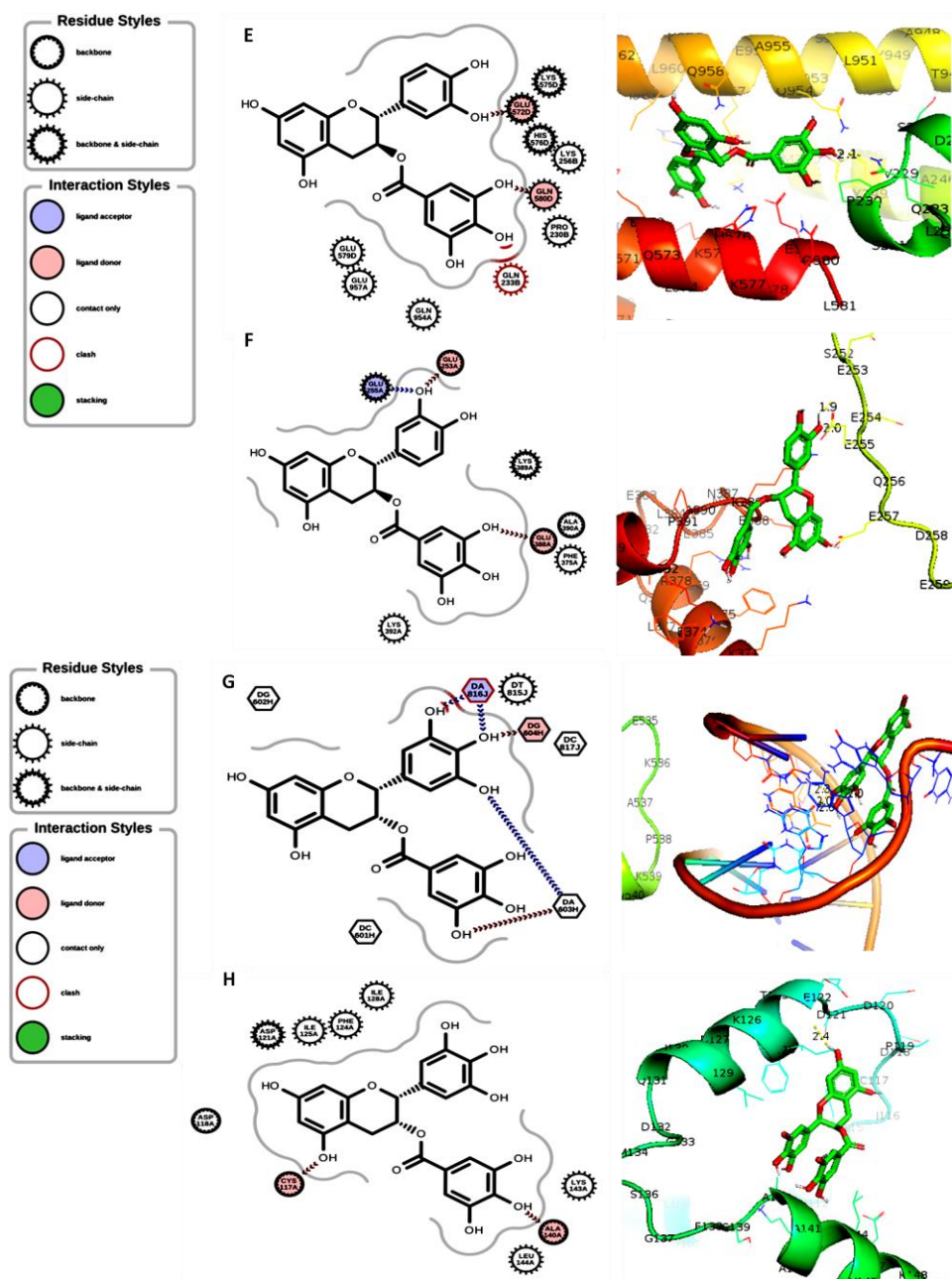


Figure 3. Interaction of the binding poses of: (A) CHEMBL284377 and c-Myc/Max; (B) Doconexent and c-Myc/Max; (C) OMH and c-Myc/Max; (D) TPO and c-Myc/Max; (E) XEG and c-Myc/Max; (F) XEG and c-Myc; (G). KDH and c-Myc/Max; (H) KDH and c-Myc.

In this study, molecular docking results showed that epicatechin-3-gallate (XEG) epigallocatechin gallate (KDH) and CHEMBL284377 (Dexfosfoserine) have the most promising effects on c-Myc/Max with binding affinity less than -5.00 kcal/mol, which was better than that of the standard compound Doconexent (-3.391 kcal/mol). A study by Yu et al. [27] reported binding affinity in a range of -3.483 to -6.596 for a novel set of c-Myc inhibitors. Additionally, Yao et al. [9] identified the small molecular inhibitor D347-2761 as a novel dual-targeting c-Myc/Max heterodimerization agent, disrupting c-Myc protein stability to repress multiple myeloma growth in vitro and in vivo by inhibiting CDK4 promoter transcriptional activity. Additionally, Trovafloxacin, Ozanimod, and Ozenoxacin were found to significantly decrease c-Myc mRNA levels and downregulate c-Myc expression [72]. Three compounds—ZINC000004654958, ZINC000004654971, and ZINC000008689961—were identified as safe drug candidates against c-Myc, showing no pi-pi interaction [29].

In this study, the results showed some interaction with amino acid residues and nucleotide bases in the c-Myc/Max structure. CHEMBL284377, Doconexent, TPO, and KDH bind to c-Myc/Max on the DNA helix bases, not amino acids, whereas OMH and XEG bind to c-Myc/Max on the amino acids, not DNA helix bases. These results revealed two mechanisms by which the inhibitors could interact with c-Myc/Max complex as catalytic inhibitors and c-Myc/Max poisons (DNA- and non-DNA intercalating agents) in a similar manner to the topoisomerase II alpha inhibition mechanism [73]. The Myc-Max complex structure (PDB: 1NKP) encompasses amino acids 947–980 of Myc (chain A) and 247–280 of Max (chain B), corresponding to the leucine zipper region [25,74]. A well-defined binding pocket, constituted by specific residues in both c-Myc and Max (Leu917, Phe921, and Lys939 in c-Myc and Arg212, Arg215, Asp216, Ile218, Lys219, Phe222, and Arg239 in Max), has been identified as the binding site for c-Myc inhibitors [75]. Ligand interaction analysis of seven compounds with c-Myc/Max highlighted key residues shaping the neighborhood of the hot spot and warm spot residues [30]. A study has shown that compound PKUMDL-YC-1205 binds to the Holo conformation of c-Myc by interacting with Arg372 and Ser373 [27], and compound 10074-G5 interacts with Arg366, Arg367, and Arg372 [76].

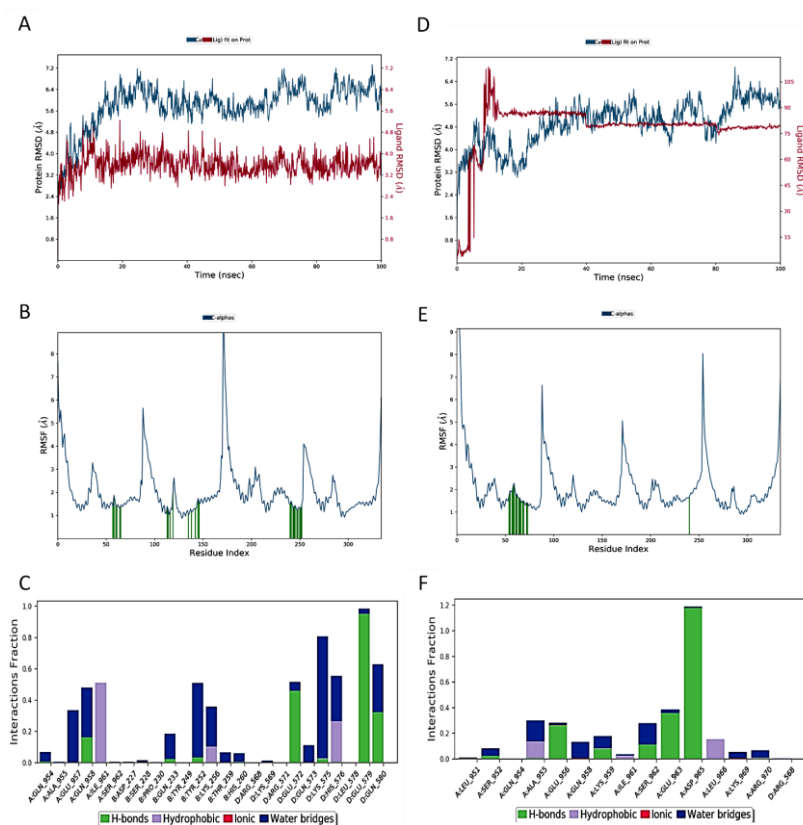


Figure 4. Protein-ligand complex simulation results (A) RMSD of c-Myc/Max – XEG; (B) RMSF of c-Myc/Max; (C) Interaction profile of the contact between c-Myc/Max – XEG; (D) RMSD of c-Myc/Max – KDH; (E) RMSF of c-Myc/Max; (F) Interaction profile of the contact between c-Myc/Max – KDH.

MD simulations were employed to evaluate the structural stability of the protein and the binding status of the ligand in a physiologically relevant environment. For ease of comparison, the c-Myc/Max binding complexes with compounds XEG and KDH were utilized for MDS analysis. The results, depicted in Figure 4(a-f), provide valuable insights into the dynamic behavior and interactions of the protein-ligand complexes under realistic conditions. The RMSD of c-Myc/Max binding with XEG showed a protein RMSD of 7.0 Å and a ligand RMSD of 4.80 Å from 0 to 100 ns (Figure 4a). The RMSF of c-Myc/Max peaked at amino acid

residues 80-100, 165-175, and 250-260 (Figure 4b). Details about hydrophobic interactions, hydrogen bonds, water bridges, and ionic interactions in the protein-ligand interactions are illustrated in Figure 4c. In contrast, the RMSD of KDH binding with c-Myc/Max indicated a protein RMSD of 7.0 Å and a concerning ligand RMSD of 100 Å from 0 to 100 ns (Figure 4d). The RMSF of c-Myc/Max exhibited significant fluctuations at amino acid residues 80-100, 165-175, and 250-260 (Figure 4e). The protein-ligand interactions, including details on hydrophobic interactions, hydrogen bonds, water bridges, and ionic interactions, are presented in Figure 4f. The result of MD simulation showed suitable protein-ligand stability and interactions of c-Myc/Max and XEG with GLU957, ILE961, GLU572, LYS575, GLU597, and TYR252 as major amino acid residues, while c-Myc/Max and KDH interaction have GLU956 and ASP965 as major amino acid residues. A schematic of detailed ligand atom interactions with the protein residues is presented in Figure 5.

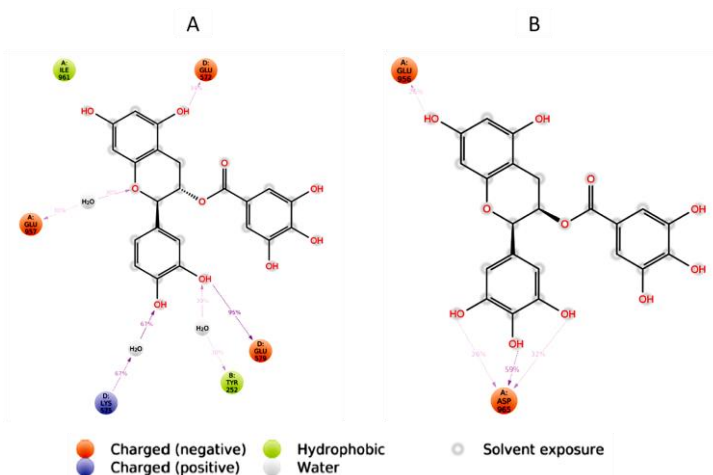


Figure 5. A schematic of detailed ligand-protein interactions (A) c-Myc/Max with XEG; (B) c-Myc/Max with KDH.

MD simulation was employed to assess atomic-level variations in the protein-ligand system and evaluate the stability of the complex in a dynamic environment [39]. MD simulation calculates the trajectory of atoms over time, enabling the study of various processes, such as structural variation and ligand-protein contact [64]. The RMSD is usually used to assess flexibility, compactness, and conformational divergence, with RMSD values less than 4 Å indicating relatively small conformational changes and suggesting stability during simulation [40]. The RMSD of c-Myc of about 16 Å has been reported to show that the structure gains a stable conformation during about 410 ns simulation, with ligands interacting with residues Val953, Gln954, Glu956, and Glu957 [30].

Table 4. Binding energy (ΔG^{bind}) of the interaction of c-Myc/Max with XEG and KDH, respectively, at 0 and 100 ns.

Complex	Simulation Time (ns)	MMGBSA ΔG (kcal.mol ⁻¹)							ΔG^{bind} (Total)
		Coulomb	Covalent	Hbond	Lipo	Packing	Solv_GB	vdW	
XEG - c-Myc/Max	0	-27.567	5.940	-2.13737	-10.795	-1.200	26.652	-34.553	-43.661
	100	-18.304	4.217	-2.54325	-9.613	-1.903	18.495	-38.820	-48.470
KDH - c-Myc/Max	0	-56.999	1.032	0	-4.979	-1.387	52.595	-20.999	-30.737
	100	-7.636	-1.640	0	-1.123	0	8.162	-1.741	-3.977

Legend: **Total:** Total binding energy (Prime energy). **Lipo:** Lipophilic energy. **Covalent:** Covalent binding energy. **Packing:** Pi-pi packing correction **Hbond:** Hydrogen bonding energy. **Coulomb:** Coulomb energy. **Solv GB:** Generalized Born electrostatic solvation energy. **vdW:** Van der Waals energy.

The binding free energies for all complexes were computed using MMGBSA at both 0 ns and 100 ns time points, as shown in Table 4. The results indicate that the binding energy ΔG_{bind} (Total) for XEG - c-Myc/Max complex at 0 ns and 100 ns were -43.661 and -48.470 kcal/mol, respectively, while binding energy ΔG_{bind} (Total) for KDH - c-Myc/Max complex at 0 ns and 100 ns were -30.737 and -3.977 kcal/mol respectively.

The result indicates that the XEG - c-Myc/Max complex is more stable in energetics than the KDH - c-Myc/Max complex during the 100 ns MD simulation. Prime MM-GBSA provided various energy properties, including ligand, receptor, complex energies, and energy differences related to strain and binding [40]. The results of MMGBSA binding energy in this study showed that the XEG - c-Myc/Max complex possessed stabilized Van der Waals energy, Coulomb energy, and solvation energy, while the KDH - c-Myc/Max complex has unstable Coulomb energy, solvation energy, and Van der Waals energy, in simulated physiological condition. This difference may account for the mechanism of catalytic inhibition and poison by intercalation, respectively, as hypothesized in this study. Previous studies reported MM-GBSA binding free energies for the Myc-Max complex using distance and position restraints, as well as MM-GBSA scores for c-Myc/Max–ligand complexes within the range of -20 to -50 kcal/mol [25,30]. These calculations provide valuable insights into the stability and energetics of the studied biomolecular systems.

4. Conclusions

The study showed potential c-Myc or c-Myc/Max modulators for cancer therapy by leveraging computational methods. Potential compounds that could selectively modulate c-Myc/Max interaction were identified, offering new avenues for drug development. Further *in vivo* investigations are imperative to validate the efficacy of CHEMBL1077108 (Furospogonide), CHEMBL464381 (Palinurin), TPO (Phosphothreonine), CHEMBL284377 (Dexfosfoserine), and XEG ((+)-Catechin 3-Gallate), in addressing various c-Myc-implicated cancer diseases, with a specific focus on multiple myeloma. This study lays the groundwork for potential therapeutic interventions targeting c-Myc and opens avenues for future research in cancer treatment.

Author Contributions

All authors have read and agreed to the published version of the manuscript.

Institutional Review Board Statement

Not applicable

Informed Consent Statement

Not applicable

Data Availability Statement

Data supporting the findings of this study are available upon reasonable request from the corresponding author.

Funding

This research received no external funding.

Acknowledgments

None.

Conflicts of Interest

The authors declare no conflict of interest.

References

1. Carabet, L.A.; Rennie, P.S.; Cherkasov, A. Therapeutic Inhibition of Myc in Cancer. Structural Bases and Computer-Aided Drug Discovery Approaches. *Int. J. Mol. Sci.* **2019**, *20*, 120, <https://doi.org/10.3390/ijms20010120>.
2. Dang, C.V.; O'Donnell, K.A.; Zeller, K.I.; Nguyen, T.; Osthus, R.C.; Li, F. The c-Myc target gene network. *Seminars Cancer Biol* **2006**, *16*, 253–264, <https://doi.org/10.1016/j.semcancer.2006.07.014>.
3. Wahlström, T.; Henriksson, M.A. Impact of MYC in regulation of tumor cell metabolism. *BBA - Gene Regulatory Mechanisms* **2015**, *1849*, 563–569, <https://doi.org/10.1016/j.bbagr.2014.07.004>.
4. Mao D.Y.; Watson JD, Yan PS, Barsyte-Lovejoy, D.; Khosravi, F.; Wong, W.W.; Farnham, P. J.; Huang, T. H.; Penn, L.Z. Analysis of Myc bound loci identified by CpG island arrays shows that Max is essential for Myc-dependent repression. *Curr Biol* **2003**, *13*, 882–886, [https://doi.org/10.1016/s0960-9822\(03\)00297-5](https://doi.org/10.1016/s0960-9822(03)00297-5).
5. Sabo, A.; Kress, T.R.; Pelizzola, M.; de Pretis, S.; Gorski, M.M.; Tesi, A.; Morelli, M.J.; Bora, P.; Doni, M.; Verrecchia, A.; Tonelli, C.; Fagà, G.; Bianchi, V.; Ronchi, A.; Low, D.; Müller, H.; Guccione, E.; Campaner, S.; Amati, B.. Selective transcriptional regulation by Myc in cellular growth control and lymphomagenesis. *Nature* **2014**, *511*, 488–492, <https://doi.org/10.1038/nature13537>.
6. Thomas, L.; Wang, Q.; Grieb, B.; Phan, J.; Foshage, A.; Sun, Q.; Olejniczak, E.; Clark, T.; Dey, S.; Lorey, S.; Alicie, B.; Howard, G.; Cawthon, B.; Ess, K.; Eischen, C.; Zhao, Z.; Fesik, S.; Tansey, W. Interaction with WDR5 Promotes Target Gene Recognition and Tumorigenesis by MYC. *Molecular Cell* **2015**, *58*, 440–452, <https://doi.org/10.1016/j.molcel.2015.02.028>.
7. Seoane, J.; Pouponnot, C.; Staller, P.; Schader, M.; Eilers, M.; Massagué, J. TGFbeta influences Myc, Miz-1 and Smad to control the CDK inhibitor p15INK4b. *Nature Cell Biology* **2001**, *3*, 400–408, <https://doi.org/10.1038/35070086>.
8. García-Gutiérrez, L.; Delgado, M.D.; León, J. MYC Oncogene Contributions to Release of Cell Cycle Brakes. *Genes* **2019**, *10*, 244, <https://doi.org/10.3390/genes10030244>.
9. Yao, R.; Zhang, M.; Zhou, J.; Liu, L.; Zhang, Y.; Gao, J.; Xu, K. Novel dual-targeting c-Myc inhibitor D347-2761 represses myeloma growth via blocking c-Myc/Max heterodimerization and disturbing its stability. *Cell Comm Signal* **2022**, *20*, 73, <https://doi.org/10.1186/s12964-022-00868-6>.
10. Branagan, A.; Lei, M.; Lou, U.; Raje, N. Current Treatment Strategies for Multiple Myeloma. *JCO Oncol Pract* **2020**, *16*, 5–14, <https://doi.org/10.1200/JOP.19.00244>.
11. Gulla, A.; Anderson, K.C. Multiple myeloma: the (r)evolution of current therapy and a glance into the future. *Haematologica* **2020**, *105*, 2358–2367, <https://doi.org/10.3324/haematol.2020.247015>.
12. Morè, S.; Corvatta, L.; Manieri, V.M.; Morsia, E.; Poloni, A.; Offidani, M. Novel Immunotherapies and Combinations: The Future Landscape of Multiple Myeloma Treatment. *Pharmaceuticals* **2023**, *16*, 1628, <https://doi.org/10.3390/ph16111628>.
13. Holien, T.; Vatsveen, T.K.; Hella, H.; Waage, A.; Sundan, A. Addiction to c-MYC in multiple myeloma. *Blood* **2012**, *120*, 2450–2453, <https://doi.org/10.1182/blood-2011-08-371567>.
14. Gupta, M.; Pal, R.A.G.K.; Tikoo, D. Multiple myeloma: the disease and its treatment. *Int J Basic Clin Pharmacol* **2013**, *2*, 103–121, <https://doi.org/10.5455/2319-2003.ijbcp20130302>.
15. Moreau, P.; Sonneveld, P.; Boccadoro, M.; Cook, G.; Mateos, M.V.; Nahi, H.; Goldschmidt, H.; Dimopoulos, M.A.; Lucio, P.; Bladé, J.; Delforge, M.; Hajek, R.; Ludwig, H.; Facon, T.; Miguel, J. F. S.; Einsele, H. Chimeric antigen receptor T-cell therapy for multiple myeloma: a consensus statement from The European Myeloma Network. *Haematologica* **2019**, *104*, 2358–2360, <https://doi.org/10.3324/haematol.2019.224204>.

16. Richardson PG, Siegel DS, Vij R; Hofmeister, C.C.; Baz, R.; Jagannath, S.; Chen, C.; Lonial, S.; Jakubowiak, A.; Bahlis, N.; Song, K.; Belch, A.; Raje, N.; et al. Pomalidomide alone or in combination with low-dose dexamethasone in relapsed and refractory multiple myeloma: a randomized phase 2 study. *Blood* **2014**, *123*, 1826–1832, <https://doi.org/10.1182/blood-2013-11-538835>.
17. Shah, N.; Chari, A.; Scott, E.; Mezzi, K.; Usmani, S.Z.. B-cell maturation antigen (BCMA) in multiple myeloma: rationale for targeting and current therapeutic approaches. *Leukemia* **2020**, *34*, 985–1005, <https://doi.org/10.1038/s41375-020-0734-z>.
18. Kiessling, A.; Sperl, B.; Hollis, A.; Eick, D.; Berg, T. Selective Inhibition of c-Myc/Max Dimerization and DNA Binding by Small Molecules. *Chem Biol* **2006**, *13*, 745–751, <https://doi.org/10.1016/j.chembiol.2006.05.011>.
19. Chen, H.; Liu, H.; Qing, G. Targeting oncogenic Myc as a strategy for cancer treatment. *Signal Transduct Target Therap* **2018**, *3*, 5, <https://doi.org/10.1038/s41392-018-0008-7>.
20. Duffy, M.J.; O’Grady, S.; Tang, M.; Crown, J. MYC as a target for cancer treatment. *Cancer Treat Rev* **2021**, *94*, 102154, <https://doi.org/10.1016/j.ctrv.2021.102154>.
21. Llombart, V.; Mansoura, M.R. Therapeutic targeting of “undruggable” MYC. *eBioMedicine* **2022**, *75*, 103756, <https://doi.org/10.1016/j.ebiom.2021.103756>.
22. Huang, H.; Weng, H.; Wang, L.; Yu, C.; Huang, Q.; Zhao, P.; Wen, J.; Zhou, H.; Qu, L. Triggering Fbw7-Mediated Proteasomal Degradation of c-Myc by Oridonin Induces Cell Growth Inhibition and Apoptosis. *Mol Cancer Therapeut* **2012**, *11*, 1155–1165, <https://doi.org/10.1158/1535-7163.MCT-12-0066>.
23. Wiegering, A.; Uthe, F.W.; Jamieson, T.; Ruoss, Y.; Hüttenrauch, M.; Küspert, M.; Pfann, C.; Nixon, C.; Herold, S.; Walz, S.; Taranets, L.; Germer, C.; Rosenwald, A.; Sansom, O.J.; Eilers, M. Targeting Translation Initiation Bypasses Signaling Crosstalk Mechanisms That Maintain High MYC Levels in Colorectal Cancer. *Cancer Discov* **2015**, *5*, 768–781, <https://doi.org/10.1158/2159-8290.CD-14-1040>.
24. Jain, S.; Wang, X.; Chang, C.; Ibarra-Drendall, C.; Wang, H.; Zhang, Q.; Brady, S.W.; Li, P.; Zhao, H.; Dobbs, J.; Kyrish, M.; Tkaczyk, T.S.; Ambrose, A.; Sistrunk, C.; Arun, B.K.; Richards-Kortum, R.; Jia, W.; Seewaldt, V.L.; Yu, D. Src Inhibition Blocks c-Myc Translation and Glucose Metabolism to Prevent the Development of Breast Cancer. *Cancer Research*. **2015**, *75*, 4863–4875, <https://doi.org/10.1158/0008-5472.CAN-14-2345>.
25. Jouaux, E.M.; Timm, B.B.; Arndt, K.M.; Exnerd, T.E. Improving the interaction of Myc-interfering peptides with Myc using molecular dynamics Simulations. *J. Pept. Sci.* **2009**, *15*, 5–15, <https://doi.org/10.1002/psc.1078>.
26. Mustata, G.; Follis, A.V.; Hammoudeh, D.I.; Metallo, S.J.; Wang, H.; Prochownik, E.V.; Lazo J.S.; Bahar I. (2009). Discovery of Novel Myc-Max Heterodimer Disruptors with a Three-Dimensional Pharmacophore Model. *J. Med. Chem* **2009**, *52*, 1247–1250, <https://doi.org/10.1021/jm801278g>.
27. Yu, C.; Niu, X.; Jin, F.; Liu, Z.; Jin, C.; Lai, L. Structure-based Inhibitor Design for the Intrinsically Disordered Protein c-Myc. *Scientific Reports*, **2016**, *6*, 22298, <https://doi.org/10.1038/srep22298>.
28. Castell, A.; Yan, Q.; Fawkner, K.; Hydbring, P.; Zhang, F.; Verschut, V.; Franco, M.; Zakaria, S. M.; Bazzar, W.; Goodwin, J.; Zinzalla, G.; Larsson, L.G. A selective high affinity MYC-binding compound inhibits MYC: MAX interaction and MYC-dependent tumor cell proliferation. *Sci. Rep* **2018**, *8*, 10064–10081, <https://doi.org/10.1038/s41598-018-28107-4>.
29. Ren, J.; Huangfu, Y.; Ge, J.; Wu, B.; Li, W.; Wang, X.; Zhao, L. Computational study on natural compounds inhibitor of c-Myc. *Medicine* **2020**, *99*, e23342, <https://doi.org/10.1097/MD.00000000000023342>.
30. Singh, A.; Kumar, P.; Sarvagalla, S.; Bharadwaj, T.; Nayak, N.; Coumar, M.S.; Giri, R.; Garg, N. Functional inhibition of c-Myc using novel inhibitors identified through “hot spot” targeting. *J. Biol. Chem* **2022**, *298*, 101898, <https://doi.org/10.1016/j.jbc.2022.101898>.
31. Zhou, Y.; Gao, X.; Yuan, M.; Yang, B.; He, Q.; Cao, J. Targeting Myc Interacting Proteins as a Winding Path in Cancer Therapy. *Front. Pharmacol* **2021**, *12*, 748852, <https://doi.org/10.3389/fphar.2021.748852>.
32. Szklarczyk, D.; Gable, A.L.; Nastou, K.C.; Lyon, D.; Kirsch, R.; Pyysalo, S.; Doncheva, N.T.; Legeay, M.; Fang, T.; Bork, P.; Jensen, L.J.; von Mering, C. The STRING database in 2021: Customizable protein–protein networks, and functional characterization of user-uploaded gene/measurement sets. *Nucleic Acids Res.* **2021**, *49*, D605–D612, <https://doi.org/10.1093/nar/gkaa1074>.
33. Radusky, L.; Ruiz-Carmona, S.; Modenutti, C.; Barril, X.; Turjanski, A.G.; Martí, M.A. LigQ: A Webserver to Select and Prepare Ligands for Virtual Screening. *J. Chem. Inf. Model* **2017**, *57*, 1741–1746, <https://doi.org/10.1021/acs.jcim.7b00241>.

34. Backman, T.W.H.; Cao, Y.; Girke, T. ChemMine tools: an online service for analyzing and clustering small molecules. *Nucleic Acids Res* **2011**, *39*, W486–W491, <https://doi.org/10.1093/nar/gkr320>.
35. Daina, A.; Michielin, O.; Zoete, V. (2017) SwissADME: a free web tool to evaluate pharmacokinetics, drug-likeness and medicinal chemistry friendliness of small molecules. *Sci Rep* **2017**, *7*, 42717, <https://doi.org/10.1038/srep42717>.
36. Morris, G.M.; Huey, R.; Lindstrom, W.; Sanner, M.F.; Belew, R.K.; Goodsell, D.S.; Olson, A.J. AutoDock4 and AutoDockTools4: automated docking with selective receptor flexibility. *J. Comput. Chem* **2009**, *30*, 2785–2791, <https://doi.org/10.1002/jcc.21256>.
37. Trott, O.; Olson, A.J. AutoDock Vina: improving the speed and accuracy of docking with a new scoring function, efficient optimization, and multithreading. *J. Comput. Chem* **2010**, *31*, 455–461, <https://doi.org/10.1002/jcc.21334>.
38. Eberhardt, J.; Santos-Martins, D.; Tillack, A.F.; Forli, S. AutoDock Vina 1.2.0: New Docking Methods, Expanded Force Field, and Python Bindings, *J. Chem. Inf. Model* **2021**, *61*, 3891–3898, <https://doi.org/10.1021/acs.jcim.1c00203>.
39. Fatoki, T.H.; Balogun, C.T.; Oluwadare, O.T.; Famusiwa, C.D.; Oyebiyi, O.R.; Ejimadu, B.A.; Lawal, O.E.; Amosun, B.E.; Adeyeye, T.O.; Falode, J.A. *In Silico* Evaluation of Nutri-Pharmacological Potentials of Phytochemicals in Sorghum (*Sorghum bicolor*) Grains. *J. Food Bioact* **2023**, *23*, <https://doi.org/10.31665/JFB.2023.18354>.
40. Fatoki, T.H.; Faleye, B.C.; Nwagwe, O.R.; Awofisayo, O.A.; Adeseko, C.J.; Jeje, T.O.; Ayenero, M.E.; Fatoki, J.M.; Akinlolu, O.S.; Momodu, D.U.; Enibukun, J.S.; Omuekwu, N.F. Friedelin Could Moderately Modulate Human Carbonic Anhydrases: An *in Silico* Study. *Biointer Res Appl Chem* **2024**, *14*, 49, <https://doi.org/10.33263/BRIAC142.049>.
41. Tao, A.; Huang, Y.; Shinohara, Y.; Caylor, M.L.; Pashikanti, S.; Xu, D. ezCADD: A Rapid 2D/3D Visualization-Enabled Web Modeling Environment for Democratizing Computer-Aided Drug Design. *J. Chem. Inf. Model.* **2019**, *59*, 18–24, <https://doi.org/10.1021/acs.jcim.8b00633>.
42. Ali, I.; Iqbal, M.N.; Ibrahim, M.; Haq, I.U.; Alonazi, W.B.; Siddiqi, A.R. Computational exploration of novel ROCK2 inhibitors for cardiovascular disease management; insights from high-throughput virtual screening, molecular docking, DFT and MD simulation. *PLoS ONE* **2023**, *18*, e0294511, <https://doi.org/10.1371/journal.pone.0294511>.
43. Schrödinger. Schrödinger release 2018-3. Desmond molecular dynamics system, D.E. Shaw research, New York, NY, 2018. Maestro Desmond Interoperability Tools, Schrödinger, New York, NY, **2018**.
44. Fatoki, T.H. Effect of pH on structural dynamics of HMGCoA reductase and binding affinity to β -sitosterol. *J. Biomol. Struct. Dyn* **2023**, *41*, 4398-4404, <https://doi.org/10.1080/07391102.2022.2067240>.
45. Schrödinger. What do all the Prime MM-GBSA energy properties mean?. **2019**. Available online: www.schrodinger.com/kb/1875 Accessed on March 5, 2024.
46. Zhang, N.; Ichikawa, W.; Faiola, F.; Lo, S.; Liu, X.; Martinez, E. MYC interacts with the human STAGA coactivator complex via multivalent contacts with the GCN5 and TRRAP subunits. *BBA – Gene Regulat Mech* **2014**, *1839*, 395-405, <https://doi.org/10.1016/j.bbagr.2014.03.017>.
47. Faiola F., Liu X., Lo S., Pan S., Zhang K., Lyman E., Farina A.; Martinez E.. Dual Regulation of c-Myc by p300 via AcetylationDependent Control of Myc Protein Turnover and Coactivation of Myc-Induced Transcription. *Mol Cell Biol* **2005**, *25*, 10220-10234, <https://doi.org/10.1128/MCB.25.23.10220-10234.2005>.
48. Austen, M.; Vervoorts, J.; Lüscher-Firzlaff, J.M.; Rottmann, S.; Lilischkis, R.; Lüscher, B.; Dohmann, K.; Walsemann, G. Stimulation of c-MYC transcriptional activity and acetylation by recruitment of the cofactor CBP. *EMBO Reports*. **2003**, *4*, 484-490, <https://doi.org/10.1038/sj.embor.embor821>.
49. Fiorentino, F.P.; Tokgün, E.; Solé-Sánchez, S.; Giampaolo, S.; Tokgün, O.; Jauset, T.; Kohno, T.; Perucho, M.; Soucek, L.; Yokota, J. Growth suppression by MYC inhibition in small cell lung cancer cells with TP53 and RB1 inactivation. *Oncotarget* **2016**, *7*, 31014–31028, <https://doi.org/10.18632/oncotarget.8826>.
50. Bello-Fernandez, C.; Packham, G.; Cleveland, J.L. The ornithine decarboxylase gene is a transcriptional target of c-Myc. *Proc Natl Acad Sci USA* **1993**, *90*, 7804–7808, <https://doi.org/10.1073/pnas.90.16.7804>.
51. Wu, K.J.; Polack, A.; Dalla-Favera, R. Coordinated regulation of iron-controlling genes, H-ferritin and IRP2, by c-MYC. *Science* **1999**; *283*, 676–679, <https://doi.org/10.1126/science.283.5402.676>.
52. Gomez-Roman, N.; Grandori, C.; Eisenman, R.N.; White, R.J. Direct activation of RNA polymerase III transcription by c-Myc. *Nature* **2003**, *421*, 290–294, <https://doi.org/10.1038/nature01327>.

53. Lin, C.; Lovén, J.; Rahl, P.; Paranal, R.; Burge, C.; Bradner, J.; Lee, T.; Young, R. Transcriptional Amplification in Tumor Cells with Elevated c-Myc. *Cell* **2012**, *151*, 56-67, <https://doi.org/10.1016/j.cell.2012.08.026>.
54. Pelengaris, S.; Khan, M.; Evan, G. c-MYC: more than just a matter of life and death. *Nat Rev Cancer* **2002**, *2*, 764–776, <https://doi.org/10.1038/nrc904>.
55. Morrish, F.; Giedt, C.; Hockenbery, D. c-MYC apoptotic function is mediated by NRF-1 target genes. *Genes Dev* **2003**, *17*, 240–255, <https://doi.org/10.1101/gad.1032503>.
56. Gabay, M.; Li, Y.; Felsner, D.W. (2014) MYC Activation Is a Hallmark of Cancer Initiation and Maintenance. *Cold Spring Harbor Perspect Med* **2014**, *4*, a014241, <https://doi.org/10.1101/cshperspect.a014241>.
57. Staller, P.; Peukert, K.; Kiermaier, A.; Seoane, J.; Lukas, J.; Karsunky, H.; Möröy, T.; Bartek, J.; Massagué, J.; Hänel, F.; Eilers, M. Repression of p15INK4b expression by Myc through association with Miz-1. *Nat Cell Biol* **2001**, *3*, 392–399, <https://doi.org/10.1038/35070076>.
58. Dang, C.V.; Reddy, E.P.; Shokat, K.M.; Soucek, L. Drugging the 'undruggable' cancer targets. *Nat Rev Cancer* **2017**, *17*, 502-508, <https://doi.org/10.1038/nrc.2017.36>.
59. Bretones, G.; Delgado, M.D.; León, J. Myc and cell cycle control. *BBA – Gene Reg Mech* **2015**, *1849*, 506-516, <https://doi.org/10.1016/j.bbagr.2014.03.013>.
60. Kim, J.; Zhang, X.; Rieger-Christ, K.M.; Summerhayes, I.C.; Wazer, D.E.; Paulson, K.E.; Yee, A.S. Suppression of Wnt Signaling by the Green Tea Compound (-)-Epigallocatechin 3-Gallate (EGCG) in Invasive Breast Cancer Cells. *J Biol Chem* **2006**, *281*, 10865–10875, <https://doi.org/10.1074/jbc.M513378200>.
61. Posternak, V.; Cole, M.D. Strategically targeting MYC in cancer. *FI000Research* **2016**, *5*, 408, <https://doi.org/10.12688/fi000research.7879.1>.
62. Whitfield, J.R.; Beaulieu, M.; Soucek, L. Strategies to Inhibit Myc and Their Clinical Applicability. *Frontiers Cell Develop Biol* **2017**, *5*, 10, <https://doi.org/10.3389/fcell.2017.00010>.
63. Wang, H.; Hammoudeh, D.I.; Follis, A.V.; Reese, B.E.; Lazo, J.S., Metallo, S.J.; Prochownik, E.V. Improved low molecular weight Myc-Max inhibitors. *Mol Cancer Therapeut* **2007**, *6*, 2399–2408, <https://doi.org/10.1158/1535-7163.MCT-07-0005>.
64. Ajayi, I.I.; Fatoki, T.H.; Alonge, A.S.; Famusiwa, C.D.; Saliu, I.O.; Akinlolu, O.S.; Onodugo, C.A.; Ojo, R.T. *In silico* ADME and molecular simulation studies of pharmacological activities of phytoconstituents of *Annona muricata* (L.) Fruit. *J. Food Bioact* **2024**, <https://doi.org/10.31665/JFB.2024.18374>.
65. Sullivan, S.S. Unravelling the molecular dynamics of c-MYC's TAD domain: a journey from simulation optimisation to drug discovery. Doctoral thesis, Department of Life Sciences, Imperial College London, London. **2021**, 1-152.
66. Liu, Y.; Liu, R.; Mao, S.C.; Morgan, J.B.; Jakobsons, M.B.; Zhou, Y.D.; Nagle, D.G. Molecular-targeted antitumor agents. 19. Furospongolide from a Marine *Lendenfeldia* sp. Sponge inhibits hypoxia-inducible factor-1 activation in breast tumour cells. *J Nat Prod* **2008**, *71*, 1854–1860, <https://doi.org/10.1021/np800342s>.
67. Bidon-Chanal, A.; Feurtes, A.; Alonso, D.; Perez, D.I.; Martinez, A.; Luque, F.J.; Medina, M. Evidence for a new binding mode to GSK-3: Allosteric regulation by the marine compound palinurin. *Eur. J. Med. Chem* **2013**, *60*, 479–489, <https://doi.org/10.1016/j.ejmech.2012.12.014>.
68. Saha, P.; Banerjee, S.; Ganguly, C.; Manna, S.; Panda, C.K.; Das, S. Black tea extract can modulate protein expression of H-ras, c-Myc, p53, and Bcl-2 genes during pulmonary hyperplasia, dysplasia, and carcinoma in situ. *J Environ Pathol Toxicol Oncol*. **2005**, *24*, 211–224, <https://doi.org/10.1615/jenvpathtoxoncol.v24.i3.70>.
69. Manna, S.; Mukherjee, S.; Roy, A.; Das, S.; Panda, C.K. Tea polyphenols can restrict benzo[a]pyrene-induced lung carcinogenesis by altered expression of p53-associated genes and H-ras, c-myc and cyclin D1. *J Nutr Biochem* **2009**, *20*, 337–349, <https://doi.org/10.1016/j.jnutbio.2008.04.001>.
70. Tauber, A.L.; Schweiker, S.S.; Levonis, S.M. From tea to treatment; epigallocatechin gallate and its potential involvement in minimizing the metabolic changes in cancer. *Nutri Res* **2020**, *74*, 23-36, <https://doi.org/10.1016/j.nutres.2019.12.004>.
71. Wang, H.; Teriete, P.; Hu, A.; Raveendra-Panickar, D.; Pendelton, K.; Lazo, J.S.; Eiseman, J.; Holien, T.; Misund, K.; Oliynyk, G.; et al. Direct inhibition of c-MycMax heterodimers by celastrol and celastrol-inspired triterpenoids. *Oncotarget* **2015**, *6*, 32380–32395, <https://doi.org/10.18632/oncotarget.6116>.

72. Zhang, J.; Wang, T.; Geng, X.; Liu, L.; Gao, J. Identification of Trovafloxacin, Ozanimod, and Ozenoxacin as Potent c-Myc G-Quadruplex Stabilizers to Suppress c-Myc Transcription and Myeloma Growth. *Mol Informatics* **2022**, *41*, 2200011, <https://doi.org/10.1002/minf.202200011>.
73. Okoro, C.O.; Fatoki, T.H. A Mini Review of Novel Topoisomerase II Inhibitors as Future Anticancer Agents. *Int. J. Mol. Sci* **2023**, *24*, 2532, <https://doi.org/10.3390/ijms24032532>.
74. Jouaux, E.M.; Schmidtkunz, K.; Muller, K.M.; Arndt, K.M. Targeting the c-Myc Coiled Coil with Interfering Peptides to Inhibit DNA Binding. *J. Pept. Sci.* **2008**, *14*, 1022–1031, <https://doi.org/10.1002/psc.1038>.
75. Carabet, L.A.; Lalous, N.; Leblanc, E.; Ban, F.; Morin, H.; Lawn, S.; et al. Computer-aided drug discovery of Myc-Max inhibitors as potential therapeutics for prostate cancer. *Eur J Med Chem* **2018**, *160*, 108–119, <https://doi.org/10.1016/j.ejmech.2018.09.023>.
76. Hammoudeh, D.I.; Follis, A.V.; Prochownik, E.V.; Metallo, S.J. Multiple independent binding sites for small-molecule inhibitors on the oncoprotein c-Myc. *J Am Chem Soc* **2009**, *131*, 7390–7401, <https://doi.org/10.1021/ja900616b>.

Publisher's Note & Disclaimer

The statements, opinions, and data presented in this publication are solely those of the individual author(s) and contributor(s) and do not necessarily reflect the views of the publisher and/or the editor(s). The publisher and/or the editor(s) disclaim any responsibility for the accuracy, completeness, or reliability of the content. Neither the publisher nor the editor(s) assume any legal liability for any errors, omissions, or consequences arising from the use of the information presented in this publication. Furthermore, the publisher and/or the editor(s) disclaim any liability for any injury, damage, or loss to persons or property that may result from the use of any ideas, methods, instructions, or products mentioned in the content. Readers are encouraged to independently verify any information before relying on it, and the publisher assumes no responsibility for any consequences arising from the use of materials contained in this publication.

Supplementary Files

Table S1. SMILES of the ligands used in this study.

SN	Ligand Code	SMILES
1	YTH	<chem>C[CH](O[P](O)(O)=O)[CH](N)C(O)=O</chem>
2	TPO	<chem>C[C@H]([C@@H](C(=O)O)N)OP(=O)(O)O</chem>
3	D11	<chem>C[C@@H]([C@H](C(=O)O)N)OP(=O)(O)O</chem>
4	CHEMBL1077108	<chem>C\C=C/CC\C=C\Cc1cocc1)\C)\CCCC2=CC(=O)OC2</chem>
5	ZINC49053856	<chem>C/C(=CCC/C(=C/CCc1ccoc1)/C)/CCCC2=CC(=O)OC2</chem>
6	CHEMBL464381	<chem>CC(CC\C=C(/C)\C[C@H]1OC(=O)C(=C1O)C)\C=C\C=C(/C)\CCc2cocc2</chem>
7	CHEMBL284377	<chem>N[C@@H](COP(=O)(O)O)C(=O)O</chem>
8	SEP	<chem>C([C@@H](C(=O)O)N)OP(=O)(O)O</chem>
9	OMH	<chem>CO[P@](=O)(O)OC[C@@H](C(=O)O)N</chem>
10	CHEMBL1235482	<chem>O=CCCCC=O</chem>
11	ZINC01729593	<chem>C(CC=O)CC=O</chem>
12	PTD	<chem>C(CC=O)CC=O</chem>
13	XEG	<chem>c1cc(c(cc1[C@@H]2[C@H](Cc3c(cc(cc3O2)O)O)OC(=O)c4cc(c(c4)O)O)O)O</chem>
14	KDH	<chem>c1c(cc(c(c1O)O)O)[C@@H]2[C@@H](Cc3c(cc(cc3O2)O)O)OC(=O)c4cc(c(c4)O)O)O</chem>
15	EGG	<chem>c1c(cc(c(c1O)O)O)[C@@H]2[C@@H](Cc3c(cc(cc3O2)O)O)OC(=O)c4cc(c(c4)O)O)O</chem>